Inorg. Chem. 2017, 56, 3447−3458 DOI: 10.1021/acs.inorgchem.6b02987

Stereorigid OSSO-type Group 4 Metal Complexes in the Ring Opening Polymerization of *rac*-Lactide

Rosita Lapenta, Antonio Buonerba, Assunta De Nisi,[#] Magda Monari,[#] Alfonso Grassi, Stefano Milione,* Carmine Capacchione.

Department of Chemistry and Biology, University of Salerno, via Giovanni Paolo II, 132 Fisciano I-84084, Salerno, Italy.

Interuniversity Consortium Chemical Reactivity and Catalysis, CIRCC, via Celso Ulpiani 27, 70126 (BA), Italy

[#] *Dipartimento di Chimica G. Ciamician, Alma Mater Studiorum, Università di Bologna, via Selmi 2, Bologna, Italy*

Pre-print

*To whom correspondence should be addressed. E-mail: smilione@unisa.it

Inorg. Chem. 2017, 56, 3447−3458 DOI: 10.1021/acs.inorgchem.6b02987

Abstract

Herein we report the synthesis and the characterization of a series of group 4 metal complexes of general formula $\{OSSO_X\}M(OR)_2$ [X=R=^{t}Bu, M=Zr (**1**); X=Cumyl, M=Zr, R=^{t}Bu (**2**); X=Cumyl, M=Ti, R=^{i}Pr (**4**); X=Cumyl, M=Hf, R=^{t}Bu (**5**)] and $\{OSSO_X\}_2Zr$ [X=Cl (**3**)] supported by *ortho*-phenylene-bridged bis(phenolato) ligands ($OSSO_{tBu}$-*H* = 6,6'-((1,2-phenylene-bis-(sulfanediyl)-bis-(methylene))-bis-(2,4-di-tert-butyl-2-yl)-phenol; $OSSO_{Cum}$-*H* = 6,6'-((1,2-phenylene-bis-(sulfanediyl)-bis-(methylene))-bis-(2,4-di-phenylpropan-2-yl)-phenol; $OSSO_{Cl}$-*H* = 6,6'-((1,2-phenylene-bis-(sulfanediyl)-bis-(methylene))-bis(2,4-di-chloro-2-yl)-phenol). Complexes **1**-**5** were readily obtained by σ-bond metathesis reactions between the proligand and the appropriate homoleptic metal precursor. The reaction with $OSSO_{Cl}$ yielded the bis-ligand complex $\{OSSO_{Cl}\}_2Zr$ (**3**) regardless of the $OSSO_{Cl}$-*H*/$Zr(O^tBu)_4$ molar ratio or experimental conditions. All complexes were characterized in solution using NMR spectroscopy and, in the case of **2**, by single crystal X-ray diffraction experiments. These complexes were observed to have a *fac-fac* ligand wrapping and *cis* relationship between the other two monodentate ligands, zirconium and hafnium complexes **1**-**3** and **5** were configurationally stable, whereas titanium complex **4** was fluxional in solution at room temperature. The complexes were tested as initiators for the ring-opening polymerization of racemic-lactide showing, except **3**, moderate rates and good levels of polymerization control. Upon addition of an exogenous alcohol (isopropanol or tert-butanol) efficient binary catalytic systems were achieved. Polymerizations were well-controlled, as testified by the linear evolution of molecular weight as the polymerization progresses, narrow polydispersity indices, and molecular weights corresponding to those predicted on the basis of added alcohol equivalents. Experimental and theoretical evidences were provided that ROP reactions operate according to an activated monomer mechanism.

Pre-print

Inorg. Chem. 2017, 56, 3447−3458 DOI: 10.1021/acs.inorgchem.6b02987

Introduction

Production and after use disposal of petroleum based plastics have raised several economic and environmental concerns. In particular, sustainability of raw materials and biodegradability of discarded plastic waste have driven the quest to replace some conventional oil-based materials with green and degradable alternatives.[1] Polylactic acid (PLA), prepared from starch and composted or recycled after use, has already found wide applications as commodity polymers for short-time applications (e.g. packaging, fibers) and as engineering materials in biomedical and pharmaceutical fields for the production of resorbable surgical sutures, controlled drug release systems and scaffolds for tissue engineering.[2] The most common synthetic route for preparation of polylactide is the ring-opening polymerization (ROP) of lactide (LA), the cyclic dimer of lactic acid.[3] This reaction can be efficiently promoted by discrete Lewis acidic metal alkoxide complexes. Indeed, a large variety of metal complexes has been reported to mediate the ROP of LA with efficient control in terms of molecular weights, structures of end groups and stereoregularity.[4] Among these, group 4 metal complexes are particularly attractive thanks to their low toxicity, good control over polymerization process and the substantial activity and stability, even in the presence of protic impurities.[5] Typically, these catalysts are based on octahedral complexes featuring bi- or tetradentate phenoxo-type chelating ligands. Due to the hard Lewis acidic nature of the group 4 metal, phenoxo donors were matched with relatively hard first-row nitrogen-based donors.[5] One noteworthy case is the series of zirconium and hafnium complexes bearing a 2,2'-bipyrrolidine derived salan ligand, these complexes represent a rare example of initiators able to yield highly isotactically enriched polymers.[6]

The use of soft second-row atoms as a neutral donor groups to saturate the coordination environment of oxophilic metal center was shown to be beneficial for the catalytic activity as they can regulate the Lewis acidity of the metal center and consequently the catalytic reactivity of the metal center.[5] Kol et al. showed that tetradentate dithiodiolate supported group 4 complexes are extremely active initiators for lactide polymerization: full consumption of 300 equiv. of monomers was obtained in the melt after 17 min for the Ti complex and 1 min for the Hf-derivative.[7] Another interesting class of complexes is that of the group 4 complexes bearing tetradentate (OSSO)-type bis(phenolato) ligands, extensively studied by Okuda and coworkers.[8] These complexes efficiently initiate the ring-opening polymerization of lactide monomers in a controlled fashion. In particular syndiotactic poly(meso-LA) was obtained in polymerization of meso-lactide when the polymerization was initiated by OSSO-titanium complexes whereas heterotactically biased PLA was produced by OSSO-zirconium complexes.[8] More recently, Kol and Okuda introduced the tetradentate-dianionic iminethiobis(phenolate) {ONSO}-type ligands, and their group 4 metal

Pre-print

Inorg. Chem. 2017, 56, 3447−3458 DOI: 10.1021/acs.inorgchem.6b02987

complexes. They initially found that the selectivity can be dependent upon the fluxionality of the complex: the rigid complexes afforded isotactic PLA whereas the fluxional complexes afforded heterotactic PLA.[9] Subsequently, with a series of phenylene ONSO ligands, they have found that the tacticity is determined by the nature of the substituents on the phenolate and not by fluxionality.[10]

As part of our interest in the ring opening polymerization of cyclic esters promoted by group 4 metal complexes, we have recently reported on a new family of group 4 metal complexes supported by two bidentate thioetherphenolate ligands that showed good catalytic performances in terms of activity and control over polymerization processes.[11] In an effort to further examine the structure-activity relationships affecting the activity and the stereoselectivity of group 4 initiators, we developed new group 4 catalysts for lactide polymerization and get more insight in the parameters that control their activity. In this paper we report on the synthesis and structural characterization of a series of group 4 metal complexes supported by *ortho*-phenylene-bridged bis(phenolato) ligands and their use in the ROP of *rac*-lactide. Herein we show that the presence of a stiffer bridging link between the two phenoxo units results in a rigid coordination geometry around the metal centre with remarkable consequences on the catalytic performances.

Results and discussion

Synthesis and characterization

The OSSO ligands used in this work were prepared by nucleophilic substitution of the suitable 2-(bromomethyl)-phenol with benzene-1,2-dithiol using dry THF as solvent as reported in the *Scheme 1*.[12] In order to explore the influence of the steric or electronic properties of the ligands on the coordination and reactivity of the corresponding group 4 complexes we prepared three different ligands in which the R substituent on the phenoxo anionic donor is the *tert*-butyl group, the cumyl group or the chloride atom.

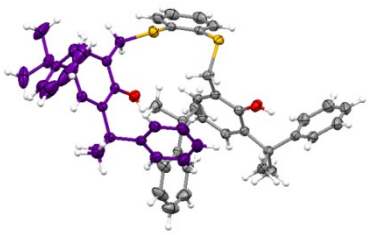

Figure 1. Molecular structure of **OSSO$_{Cum}$-*H*** in which the C atoms of one of the two sidearms of the thiophenoxo unit are depicted in purple for sake of clarity (thermal ellipsoids at the 30% probability level).

Pre-print

Inorg. Chem. 2017, 56, 3447−3458 DOI: 10.1021/acs.inorgchem.6b02987

These were purified by recrystallization or by column chromatography, and fully characterized using NMR, elemental analysis, MS, and FT-IR (see ESI). Recrystallization of $OSSO_{Cum}$-*H* from toluene afforded crystals suitable for X-ray analysis. (Figure 1)

Complexes $\{OSSO_X\}M(OR)_2$ **1-5** [X=R=^{t}Bu, M=Zr (**1**); X=Cumyl, M=Zr, R=^{t}Bu (**2**); X=Cumyl, M=Ti, R=^{i}Pr (**4**); X=Cumyl, M=Hf, R=^{t}Bu (**5**)] were prepared by σ-bond metathesis reactions between the proligand and the appropriate homoleptic metal precursor enabling alcohol elimination, in toluene solution at room temperature, as reported in the *Scheme 1*. ^{1}H NMR monitoring showed that the reactions are fast and quantitative in few minutes. In all the reaction, except that with $OSSO_{Cl}$-*H*, the desired complex of the general formula $\{OSSO_X\}M(OR)_2$ was obtained with no contamination of any side-products. Attempts to prepare the parent zirconium complex $\{OSSO_{Cl}\}Zr(O^tBu)_2$ by reacting $Zr(O^tBu)_4$ with $OSSO_{Cl}$ yielded the homoleptic complex$\{OSSO_{Cl}\}_2Zr$ (**3**) regardless of the $OSSO_{Cl}$-*H*/$Zr(O^tBu)_4$ molar ratio or experimental conditions. Reversing the order of addition of the reactants or changing the solvent (toluene or dichloromethane) or lowering the reaction temperature did not affect the outcome of the reaction. Comproportionation reaction attempts between$\{OSSO_{Cl}\}_2Zr$ and $Zr(O^tBu)_4$ did not lead to the heteroleptic complex. The homoleptic complexes $\{OSSO_{Cl}\}_2Zr$ was prepared in pure form by reacting $Zr(O^tBu)_4$ with two equivalents of the ligand precursors.

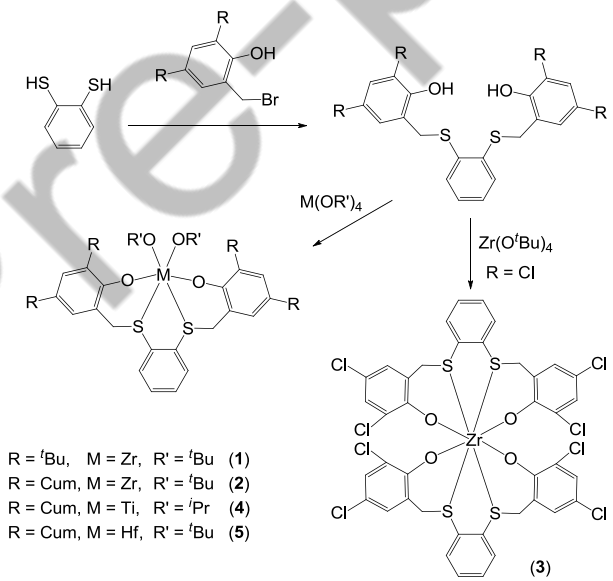

Scheme 1. Synthetic route to complexes **1-5**.

In the ^{1}H NMR spectra of complexes **1**−**5** the resonances of the OSSO ligands were unequivocally recognized and found significantly shifted with respect to the signals of the protons of free ligands. The wrapping of linear tetradentate ligands around octahedral metal centers may produce three configurational isomers designated as *mer-mer* (trans), *fac-fac* (cis-α), or *fac-mer*

Pre-print

Inorg. Chem. 2017, 56, 3447−3458 DOI: 10.1021/acs.inorgchem.6b02987

(cis-β) showing the corresponding C_{2v}, C_2, or C_1 symmetries. The last two structures are chiral-at-metal isomers and exist as two stereoisomers (Λ and Δ). In the ^{1}H NMR spectrum of **1**, a single isomer was detected. The methylene protons displayed the typical AB pattern for diastereotopic protons in C_2-symmetric environment, indicating a *fac-fac* ligand wrapping and *cis* relationship between the other two monodentate ligands. Complex **1** was configurationally stable, as matter of fact the heating of a toluene solutions up to 100 °C did not induce the coalescence of the resonances as expected for a fast Δ-Λ enantiomer interconversion but only a line broadening of the signals. This behavior is consistent with the presence of the rigid phenylene bridge between the sulfur atoms. It is worth noting that the analogous tetradentate [OSSO] zirconium complexes with the ethylene bridge and the 6−5−6 array of chelate rings is rigid at room temperature but become fluxional upon warming at 100 °C, with a coalescence temperature of 85 °C.[13] The existence of a fluxional behavior in slow exchange regime was investigated by ^{1}H–^{1}H EXSY experiment at 60 °C. As shown in Figure 2, positive cross-peaks correlating the signals of methylene groups were clearly detected. The intensity of this peak allowed us to evaluate as 0.27 s^{-1} the rate constant for the Δ-Λ interconversion, corresponding to a free energy of activation of 20.4 kcal mol^{-1}.

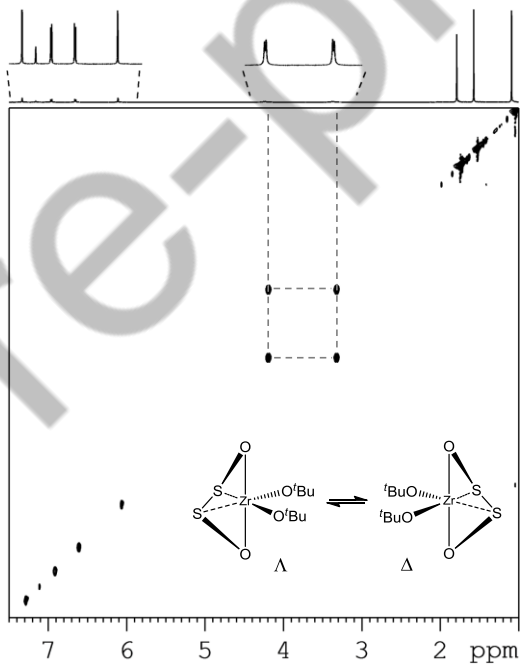

Figure 2. ^{1}H–^{1}H EXSY spectrum of $(OSSO_{tBu})Zr(O^tBu)_2$ (C_6D_6, 60 °C, mixing time = 0.400 s, 600 MHz). The exchange of the protons of the methylene group is evidenced ($k_{exchange}$ = 0.27 s^{-1}).

Single isomers of C_2-symmetry were also observed in the cases of zirconium and hafnium complexes **2** and **5**. In these cases, the symmetry of the complexes is also reflected in the spin patterns displayed by the methyl protons of the *ortho* and *para* cumyl groups. As a matter of fact

Pre-print

Inorg. Chem. 2017, 56, 3447−3458 DOI: 10.1021/acs.inorgchem.6b02987

the methyl groups of each cumyl substituent are diastereotopic and give rise to two singlets (for each cumyl group). The presence of the sterically hindered cumyl groups on the ligand skeleton increased the rigidity of the metal complexes, the rate constants for the Δ-Λ interconversion obtained from the EXSY experiments were 0.05 s^{-1} for both **2** and **5** corresponding to a free energy of activation of 21.6 kcal mol^{-1}.

The ^{1}H NMR spectrum of complex **3** was in agreement with an high symmetric structure: it featured two doublets for the eight phenoxo-CH protons (at 7.04 and 5.88 ppm) and two multiplets for the eight protons of the two phenyl bridges (at 6.59 and 6.74 ppm). The methylene protons displayed the expected AB pattern. It is worth noting that one of the two doublets was particularly downfield shifted appearing at 5.59 ppm. This prominent deshielding could be a consequence of an interaction between one proton of the S-CH_2 group with the electronegative oxygen atom of the phenoxo group. As a matter of fact, the inspection of the minimum-energy structure obtained through DFT calculation revealed a close proximity (2.46 Å) of the S-CH_2 group of one ligand to the phenoxo group of the other ligand present in the coordination sphere of the metal complexes (see Figure 3).

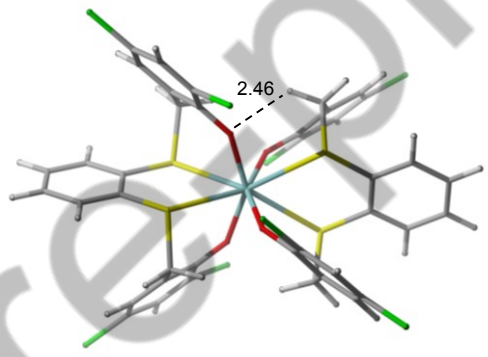

Figure 3. Minimum-energy structure for the complex **3**. The distance is given in Å.

The ^{1}H NMR spectrum of the titanium complex **4** displayed broad resonances for the S-CH_2 protons and for the methyl protons of the *ortho* cumyl groups and isopropoxide groups suggesting a fluxional C_2-symmetric structure. Even though complex **4** carries bulky cumyl groups, it is substantially more flexible than the analogous zirconium complex **2** or the less encumbered complex **1**, this behavior may be addressed to the weakening of the S-metal bonds that has to take place in this complex due to the weaker interaction between the soft sulfur atom and the hard titanium ion compared to the stronger soft-S/soft-Zr interaction. The VT NMR analysis of complex **4** showed that, at sub-ambient temperature, the resonances of methyl protons of the cumyl and isopropoxide groups as well as that of the methylene bridge broaden and resolve each in two separate peaks (Figure S13). The coalescence of the signals was observed at 0 °C, below this

Preprint

Inorg. Chem. 2017, 56, 3447−3458 DOI: 10.1021/acs.inorgchem.6b02987

temperature the resonances became sharp and well resolved and the ^{1}H NMR spectra are consistent with a slow exchange regime. Kinetic parameters were calculated using lineshape analysis of the ^{1}H NMR data measured over the temperature range -40 ÷ 30 °C in dichloromethane-d_2; ^{1}H NMR spectra and calculated exchange rates are shown in Supporting Information. The free energies of activation for the fluxional processes was calculated to be $\Delta G^{\#}$ = 13.4 ± 0.1 kcal mol^{-1} at 293 K. Activation parameters resulted to be $\Delta H^{\#}$ = 11.9 ± 0.3 kcal mol^{-1} and $\Delta S^{\#}$ = -5 ± 1 cal mol^{-1} K^{-1}.

The X-ray single crystal structure of complex (OSSO$_{Cum}$)Zr(O^{t}Bu)$_2$ (Figure 4) shows that in the solid state the C_2 symmetry is maintained if the methyl groups of the two tert-butyloxy ligands are not considered. As expected for [OSSO] and [ONNO] type complexes[14], the Zr atom possesses an octahedral environment in which the [OSSO] ligand adopts a *fac-fac* wrapping coordination mode with the tert-butyloxy ligands in mutual *cis* position. The metal atom is involved in a perfectly planar disulfometallacyclopentane ring with a S1-Zr-S2 bite angle of 70.93(2)° whereas in the two previously reported structures of [OSSO]-Zr-OtBu complexes[13,14] the Zr atom forms with the [OSSO] ligand puckered five-membered rings with wider S1-Zr-S2 bite angles 73.80(2) and 73.84(5)°. Interestingly not only the two phenolate groups in trans position are pulled away from the tert-butyloxy ligands [O1-Zr-O2 152.56(4)°] but also two terminal cumyl groups of the OSSO ligand point toward the inner thiocathecolate ring from opposite directions. The Zr-S distances [Zr-S1 2.8703(4) and Zr-S2 2.8797(4) A] are significantly longer than those found in the other two similar [(OSSO)Zr(O-tBu)$_2$] complexes [Zr-S 2.828(1) and 2.8279(7) and 2.8485(7) A][13,14] presumably in order to alleviate a worse steric congestion around the Zr atom. The Zr-O(alkoxy) and Zr-O$_{(OSSO)}$ distances fall in the range normally found for this kind of complexes.[14]

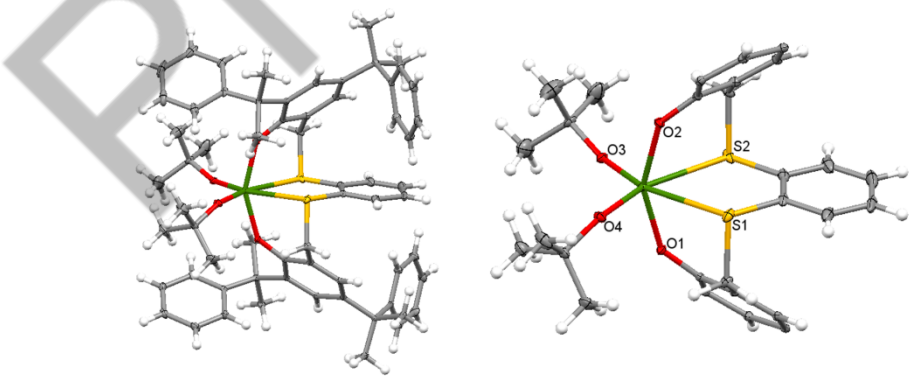

Figure 4. ORTEP drawing of (OSSO$_{Cum}$)Zr(O^{t}Bu)$_2$ showing on the left the complete structure and highlighting on the right the C_2 symmetry of the complex upon removal of the external groups (thermal ellipsoids are at 30% of the probability level). Selected bond lengths (Å) and angles (deg): Zr-S1 2.8703(6), Zr-S2 2.8797(6), Zr-O1 2.0309(14), Zr-O2 2.0380(14), Zr-O3 1.9263(14), Zr-O4 1.9420(15), S1-Zr1-S2 70.928(18).

Pre-print

Inorg. Chem. 2017, 56, 3447−3458 DOI: 10.1021/acs.inorgchem.6b02987

Ring-Opening Polymerization of *rac*-Lactide.

Complexes **1**-**5** were tested in the ROP of *rac*-lactide in toluene solution at 100 °C with a prescribed equivalent molar ratio of initiator and monomer. The main results are reported in Table 1. The reactions proceeded slowly leading to high monomer conversions in about one day, for both zirconium complexes **1** and **2**. As homoleptic group 4 metals complexes containing two (OSSO)-type ligands were found active in the ring-opening polymerization of lactide monomers,[15] we also tested complex **3**. Even after extended polymerization times, complex **3** resulted inactive. Upon changing the metal from zirconium in **2** to hafnium in **5**, the polymerization activity remained unchanged, differently, upon changing the metal from zirconium in **2** to titanium in **4**, the polymerization activity drastically decreased, satisfactory monomer conversion was achieved only after three days.

Table 1. Ring-opening polymerization of *rac*-lactide.

Entry[a]	Entry[a]	Initiator	t/h	Conv.%[b]	$M_{n(th)}$[c]	$M_{n(expt)}$[d]	PDI[d]
1	1	**1**	24	88	12.7	14.0	1.12
2	2	**2**	24	96	13.8	17.1	1.12
3	3	**3**	24	0	-	-	-
4	4	**4**	72	90	6.5[e]	6.3	1.13
5	5	**5**	24	94	13.5	15.4	1.23

[a]All reactions were carried out in 2.4 mL of toluene, $[I]_0$ = 5.0 mM, [LA] = 0.52 M, $[LA]/[I]_0$ = 100, T = 100 °C. [b]Molecular conversion determined by ^{1}H NMR spectroscopy ($CDCl_3$, 298K). [c]Calculated molecular weight using $M_{n(th)}$ (Kg mol^{-1}) = (144.13 × ($[LA]_0/[I]_0$) × LA-conversion)/1000. [d]Experimental molecular weight $M_{n(expt)}$ (Kg mol^{-1}) and polydispersity (PDI) determined by GPC in THF using polystyrene standards and corrected using the factor 0.58. [e] M_{nth} (Kg mol^{-1}) = (144.13 × ($[LA]_0/[2\times I]_0$) × LA-conversion)/1000.

In the case of the polymerization promoted by **2**, the reaction was tracked by analyzing the product mixtures sampled from the reactor at given reaction times. Each aliquot was quenched with wet $CDCl_3$ and analyzed by ^{1}H NMR spectroscopy to determine the monomer conversion. At 100 °C, an induction period of about six hours was observed, after this time the polymerization proceed with the expected first order kinetics in monomer concentration: the semilogarithmic plot was linear with a slope of 0.147 ± 0.008 h^{-1} (Figure 5a). By lowering the polymerization temperature at 80 °C, a decreases in catalytic activity (k_{obs} = 0.0371 ± 0.0009 h^{-1} see Figure 5a) and a longer induction period (about 15 hours) was observed. To get insight in this initiation/activation process, the reaction between **2** and LA in a 1:1 molar ratio was monitored by ^{1}H NMR spectroscopy. The resonances of **2** slowly disappeared together with the appearance of a very complicated new pattern

Pre-print

Inorg. Chem. 2017, 56, 3447−3458 DOI: 10.1021/acs.inorgchem.6b02987

of resonance. These NMR data suggest that the initiator **2** undergoes a drastic change, attempts to identify the product mixture were inconclusive.

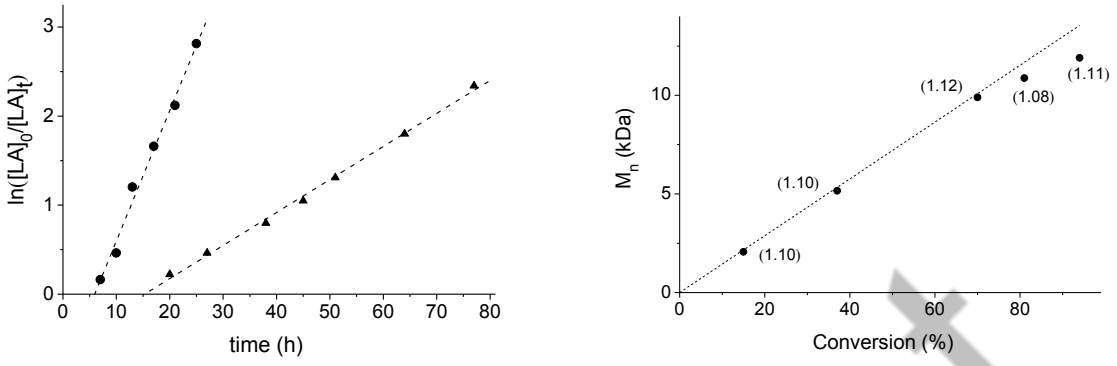

Figure 5. (a) Pseudo-first-order kinetic plot for ROP of *rac*-LA by **2** at 100 °C (●) and 80 °C (▲). (k_{obs} (100 °C) = 0.147 ± 0.008 h^{-1} R^2 = 0.986; k_{obs} (80 °C) = 0.0371 ± 0.0009 h^{-1} R^2 = 0.996). (b) Plot of number-averaged molecular weights $M_{n(expt)}$ (dot) *vs* monomer conversion (%) with theoretical $M_{n(th)}$ (dash line) using **2** as an initiator at 100 °C, M_w/M_n values are in parentheses. Conditions: $[I]_0$ = 5.0 mM; $[LA]_0/[I]_0$ = 100, toluene as solvent.)

All polymerizations led to polymers with monomodal and narrow molecular weight distributions. The molecular weights were in good agreement with the theoretical molecular weights calculated assuming the growth of one polymer chains per Mt-initiator, except for the molecular weights of the polymer by **4** for which a good correlation was obtained with the theoretical molecular weights calculated assuming the growth of two polymer chains per Ti-initiator. This behavior was previously observed in the polymerization of L-lactide promoted by other group 4 metal initiators with bi- or tetra-dentate bis(phenolato) ligands.[8a,11,16] In the case of the polymerization promoted by **2**, we verified that the experimental number average molecular weight increased linearly with the increase in the monomer conversion (Figure 5b).

The nature of the actual initiating group was investigated by NMR spectroscopy in the case of **2**. In the ^{1}H NMR spectrum in $CDCl_3$ of a relatively low molecular weight sample, a minor resonance at δ 1.46 suggested the presence of a tert-butoxycarbonyl function as terminal group (see Figure S16, Supporting Information). In the corresponding ESI-MS spectrum, the principal series of peaks was consistent with the presence of linear both even-membered and odd-membered oligomers terminated by hydroxy and tert-butoxide as chain end groups, i.e., H−[OCH(CH_3)C(=O)]$_n$−OtBu. The presence of these groups imply that the reaction is initiated by the transfer of the tert-butoxy group of the initiator to the monomer and is terminated by the hydrolysis of the metal-alkoxide bond, an observation which is indicative of a classical coordination/insertion mechanism with a ring-opening via acyloxygen bond cleavage. A second series of peaks disclosed the presence of

Pre-print

Inorg. Chem. 2017, 56, 3447−3458 DOI: 10.1021/acs.inorgchem.6b02987

cyclic oligomers. This, together with the mass-to-mass peak increment of 72 Da, indicates that intra- and inter transesterification processes are operative during the propagation step.

The microstructure of the formed PLAs was determined by homonuclear decoupled ^{1}H NMR spectra of the methane region.[17] Disappointingly, in spite of the sterorigidity of the metal complexes used as initiator, the PLAs by **1**−**5** were atactic ($P_r \approx 0.50-0.55$).

Polymerization of rac-LA in the presence of exogenous alcohol.

In the ROP of cyclic esters, the addiction of alcohol has a beneficial effect on the catalytic performance.[18] Under the so-called "immortal" polymerization conditions, alcohols can function as chain transfer agents with metal catalysts leading to the growth of one H-[PLA]-OR polymer chain per added ROH. This offers the advantage of optimizing the productivity and minimizing the contamination of polymer with metal residues. With the aim to improve our catalytic results we tested the performances of **1-5** in presence of 2-propanol, the main results are reported in Table 2.

Table 2. Ring-opening polymerization of *rac*-lactide in the presence of exogenous alcohol.

Entry[a]	Initiator	Temp.	alcohol	t/h	Conv.%[b]	$M_{n(th)}$[c]	$M_{n(expt)}$[d]	PDI[d]	P_r[e]
1	**1**	100	*i*PrOH	5	80	2.3	3.8	1.10	0.51
2	**2**	100	*i*PrOH	0.5	94	2.7	2.3	1.16	0.55
3	**2**	80	*i*PrOH	1.5	97	2.8	1.9	1.10	0.56
4	**2**	50	*i*PrOH	45	71	2.0	2.1	1.10	0.57
5	**3**	100	*i*PrOH	24	72	2.1	2.1	1.19	0.57
6	**4**	100	*i*PrOH	2	92	2.6	1.3	1.11	0.52
7	**5**	100	*i*PrOH	0.5	95	2.7	1.8	1.20	0.58
8	**2**	100	*t*BuOH	0.17	95	2.7	4.8	1.21	0.58
9	**2**	80	*t*BuOH	0.33	94	2.7	3.8	1.10	0.66
10	**2**	50	*t*BuOH	24	95	2.7	4.7	1.09	0.66

[a]All reactions were carried out in 2.4 mL of toluene, $[I]_0$ = 5.0 mM, [LA] = 0.52 M, [ROH]= 25.0 mM; $[LA]_0$:$[I]_0$:$[ROH]_0$ = 100:1:5. [b]Molecular conversion determined by ^{1}H NMR spectroscopy ($CDCl_3$, 298K). [c]Calculated molecular weight using $M_{n(th)}$ (Kg mol^{-1}) = (144.13 × ($[LA]_0$/$[ROH]_0$) × LA-conversion)/1000. [d]Experimental molecular weight $M_{n(expt)}$ (Kg mol^{-1}) and polydispersity (PDI) determined by GPC in THF using polystyrene standards and corrected using the factor 0.58. [e]Probability of racemic linkages as determined by homodecoupled ^{1}H NMR spectroscopy

To our surprise, the polymerization rates were significantly affected by the addition of isopropanol. As matter of fact, in toluene solution at 100 °C, high monomer conversions were reached in 5 hours for **1** and in half an hour for **2** and **5**. The catalytic activity increases with the increase of steric hindrance offered by the *ortho* substituents on the aromatic ring of the sulfur

Pre-print

Inorg. Chem. 2017, 56, 3447−3458 DOI: 10.1021/acs.inorgchem.6b02987

donor. This behavior was previously observed in the polymerization of L-lactide promoted by other group 4 metal initiators with a bidentate thioetherphenolate ligands.[11] In the case of the titanium complex **4** high monomer conversion was achieved in 2 hours. In presence of isopropanol also the coordinatively saturated complex **3** was effective for *rac*-lactide polymerization leading to good monomer conversion in 24 hours. Also in these cases, the formed PLA showed neither heterotactic nor isotactic enrichment. By lowering the reaction temperature at 80 or 50 °C, in the case of polymerization promoted by **2/iPrOH**, a decreases in catalytic activity was observed but the P_r values remained unaffected.

The reaction promoted by **2/iPrOH** was monitored at 80 °C by analyzing the product mixtures sampled from the reactor at certain reaction times. The monomer consumption followed a first order kinetics, with instantaneous initiation, the propagation rate constant was 2.32 ± 0.05 h^{-1}. The plot of molecular weight versus percent conversion of monomer was also obtained. A linear correlation between experimental molecular weights and percent conversion and values close to the theoretical ones calculated on the assumption of the growth of one macromolecular chain per added alcohol equivalent were observed (Figure 6a). In addition, the PDI values were relatively narrow and constant throughout the course of polymerization (Figure 6b). The ^{1}H NMR analysis of the PLA obtained in entry 2 of Table 2 clearly showed the presence of minor resonances attributable to end groups. In details, a multiplet at 5.08 ppm and a false triplet at 1.25 ppm were assigned to isopropyl ester end groups, whereas a broad multiplet at 4.35 ppm and a doublet at 1.69 ppm were assigned to the -CH(CH_3)OH end-group (see Figure S17, Supporting Information). Analysis of the ESI-MS spectrum confirmed the presence of these end groups. Also in this case the mass-to-mass peak increment of 72 Da and the presence of cyclic oligomer indicated that the polymerization process is affected by intra and intermolecular side reactions.

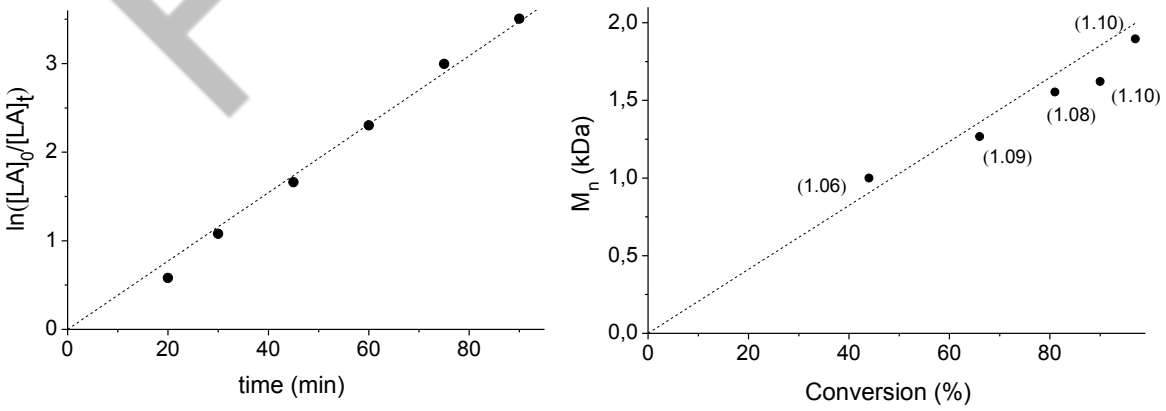

Figure 6. (a) Pseudo-first-order kinetic plot for ROP of *rac*-LA by **2**/iPrOH. (k_{obs} = 0.0386 ± 0.0008 min^{-1} = 2.32± 0.05 h^{-1}; R^2 = 0.998). (b) Plot of number-averaged molecular weights $M_{n(expt)}$ (dot) *vs* monomer conversion (%) with theoretical $M_{n(th)}$ (dash line) using **2**/iPrOH, M_w/M_n values are in parentheses. (Conditions: $[I]_0$ = 5.0 mM; $[LA]_0/[I]_0$ = 100, [iPrOH]/[I] = 5, toluene as solvent; T = 80 °C.)

Pre-print

Inorg. Chem. 2017, 56, 3447−3458 DOI: 10.1021/acs.inorgchem.6b02987

To further investigate the catalytic performances of **2**, the influence of monomer-to-initiator ratio on the polymerization was explored. The catalytic system **2**/iPrOH was able to polymerize *rac*-LA at a high loading of monomer. The number-average molecular weights of the resulting PLA increased linearly with the monomer to initiator ratio ranging from 100 to 1000 while the molecular weight distributions remained almost unchanged (see Figure 7). The line of least-squares best fit gave a gradient 19.8 g mol^{-1} (R^2 = 0.986), a value lower than the expected value of 28.8 g mol^{-1} for one chain growing per added alcohol equivalent. The mismatch between the experimental and expected molecular weights indicates a loss of control over the polymerization provided by this system at high monomer-to-initiator ratio.

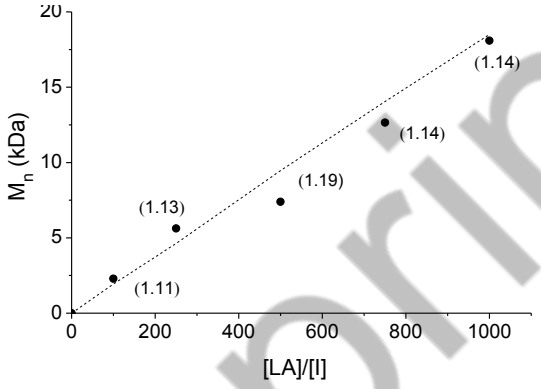

Figure 7. Plot of number-averaged molecular weights $M_{n(expt)}$ (dot) *vs* monomer to initiator ratio with theoretical $M_{n(th)}$ (dash line) using **2**/iPrOH, M_w/M_n values are in parentheses. (Conditions: $[I]_0$ = 5.0 mM; [iPrOH]/[I] = 5, toluene as solvent; T = 100 °C.)

With the acquire more insights into the mechanism of the polymerization conducted in the presence of alcohol, we monitored the reaction of this class of complexes with isopropanol. We used complex **1** for our studies as its ^{1}H NMR spectrum is quite simple. The treatment of **1** with 5 equivalent of isopropanol at room temperature in C_6D_6 resulted in the rapid exchange of the terbutoxide ligands bounded to the zirconium atom with isopropanol, yielding the isopropoxide derivative {OSSO$_{tBu}$}Zr(O*i*Pr)$_2$ (**6**) in quantitative yield. Notwithstanding a low amount (10%) of the ligand OSSO$_{tBu}$-H was initially discerned among the product mixture; over the course of 60 mins, complex **6** remained unreacted, proving that **6** is stable in presence of the residual isopropanol and the produced tert-butanol. The substitution of the alkoxide starting group on the zirconium atom may affect the rate of the initiation but, in our opinion, it hardly explains the increase of the polymerization rate that we observed when the polymerization reaction were carried out in presence of isopropanol. To clarify the role of the starting group, we thought to use tert-butanol as exogenous alcohol. First we checked the stability of **1** in presence of excess of tBuOH. The corresponding ^{1}H

Pre-print

Inorg. Chem. 2017, 56, 3447−3458 DOI: 10.1021/acs.inorgchem.6b02987

NMR spectrum was the superimposition of the NMR spectra of **1** and tBuOH taken separately. We tried to highlight the exchange between tert-butanol and **1** through an $^{1}H-^{1}H$ EXSY experiment but no crosspeak correlating the signals of tert-butanol and of the tertbutoxy group bound to the zirconium atom was detected. Addition of tert-butanol to the polymerization reaction promoted by **2** significantly affected the polymerization rate; as matter of fact high monomer conversions were achieved in about ten mins, a third of the time required using isopropanol to achieve similar conversions (compare entries 2 and 8 or 3 and 9). At 80 °C, the monomer conversion follows first-order kinetics upon monomer concentration, the apparent propagation rate constant was 7.8 ± 1.2 h^{-1}. The molecular weight increased regularly with monomer concentration and showed a good match with the theoretical ones calculated on the assumption of the growth of one macromolecular chain per added alcohol equivalent. The PDI values were narrow and constant throughout the course of polymerization. The ^{1}H NMR and ESI analysis of the PLA samples confirmed the presence of tBuOC(=O)- and -CH(CH_3)OH as end-groups.

The dependence of the polymerization rate on the nature of the exogenous alcohol and the absence of a reaction between **1** and *t*BuOH clearly indicate that the ROP reaction promoted by this class of complexes in the presence of an exogenous alcohol proceeds via the "activated monomer" mechanism.[19] In other worlds, polymerization proceeds through the attack of the alcohol (the initial added alcohol or a HO-terminated PLA chain) to the LA monomer activated by an interaction with the metal complex. Generally, in this polymerization scheme the metal complex acts as a Lewis acid catalyst.

DFT Calculations: Energy profiles of the lactide ring opening polymerization.

In order to shed more light on the "activated monomer" mechanism underlying the ring opening polymerization of lactide, a DFT investigation was carried out. To save computational resources the structural elements that are nonessential for the mechanistic understanding of the reaction were removed, *i.e.* the bulky alkyl substituents were removed from the ligand, lactide was modelled with glycolide (GL) and isopropanol was modelled with methanol. At first we tried to understand in which way the three components of our catalytic system {OSSO}Zr($OMe)_2$/MeOH/GL interact each other. We start trying to locate a coordination adduct between GL and zirconium model complex but all our attempts met with failure. The scan of the energy surface corresponding to the approach of the monomer to the zirconium atom of the complex is reported in Figure 8, it discloses a small relative minimum only when the exocyclic oxygen atom of the monomer is located at about 4.5 Å from the metal center. Relaxed optimization of the system {OSSO}Zr($OMe)_2$/GL converged to a stable adduct in which the oxygen atom of GL

Pre-print

Inorg. Chem. 2017, 56, 3447−3458 DOI: 10.1021/acs.inorgchem.6b02987

is located 4.56 Å from the metal center, this distance is not compatible with the coordination of the monomer to the metal center. A close inspection of this adduct revealed the presence of short H···O distances suggesting that GL and {OSSO}Zr(OMe)$_2$ are bounded though hydrogen-bond contacts. The binding energy (ΔH_{bind}), calculated as the difference between the enthalpy of the {OSSO}Zr(OMe)$_2$/GL adduct and the sum of the enthalpies of the metal complex {OSSO}Zr(OMe)$_2$ and the GL when they are separated, is −0.6 kcal/mol.

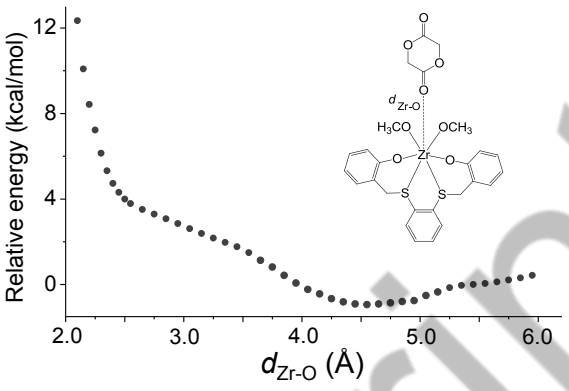

Figure 8. The potential energy surface scan for the approaching of glicolide to metal center of the zirconium model complex.

Subsequently we search for a stable coordination adduct between the zirconium model complex and methanol. In this case we succeeded in locating a stable hepta-coordinated heteroleptic derivative (***A*^{0}**) whose minimum energy structure is reported in Figure 8. In ***A*^{0}** the oxygen atom of the alcohol is located at 2.41 Å from the metal center and the hydrogen atom of the OH group points toward one of the two alcoholate ligand ($d_{H\cdots O}$=1.78 Å). The enthalpy of coordination was -4.7 kcal/mol. So we tried to coordinate the monomer on the metal center of this derivative but our attempts were unsuccessful. We only found an adduct ***A*** between ***A*^{0}** and glicolide in which the exocyclic oxygen atom of the monomer is hydrogen bonded with the OH group of the coordinated methanol ($d_{H\cdots O}$=1.79 Å), the minimum energy structure of ***A*** is reported in Figure 9.

The enthalpy change for the formation for ***A*** was -1.1 kcal/mol. We used this structure as starting point for the DFT calculations, the free energy profile is displayed in Figure 10 and the transition states are shown in Figure 11. The reaction starts with the nucleophilic attack of one of the methoxy ligands to the activated carbonyl carbon of the hydrogen bonded monomer leading to the intermediate ***B***. In this specie the hydrogen bond between the OH group and the exocyclic oxygen atom of the monomer is strengthened as the hydrogen atom is moved closer to the oxygen atom ($d_{O\cdots H}$ = 1.58 Å) while the endocyclic oxygen atom of the monomer is in close proximity to the metal center ($d_{O\cdots Zr}$ = 2.37 Å).

Pre-print

Inorg. Chem. 2017, 56, 3447−3458 DOI: 10.1021/acs.inorgchem.6b02987

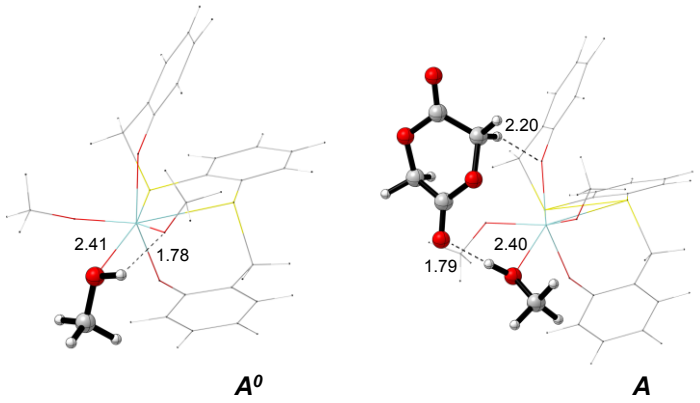

Figure 9. Minimun energy structures of adducts ***A⁰*** and ***A***. Distances are given in Å.

This step requires overcoming a barrier of 13.8 kcal/mol; this is a quite high barrier, which is however consistent with the temperature of 100 °C needed experimentally to achieve high activity. At the transition state TS_{AB}, the C=O_e bond was slightly elongated reflecting the rehybridization of C=O from sp^2 toward sp^3. Following the intrinsic reaction coordinate, intermediate ***B*** evolves toward the ring-opening transition state with an activation barrier of 4.1 kcal/mol (relative to intermediate ***B***). In TS_{BC} the proton migration was induced from the exocyclic oxygen atom to the endocyclic oxygen atom. This transition state led to the product ***C*** in which the monomer was fully opened ($C_{C=O}$–O_i = 3.76 Å). Transfer back of the hydrogen atom to the methoxy ligand and isomerization of the growing chain led to the intermediate ***D***. The formation of ***D*** featuring an heterocyclic Zr lactate makes ring opening of the monomer thermodynamically viable (-2.5 $kcalmol^{-1}$).

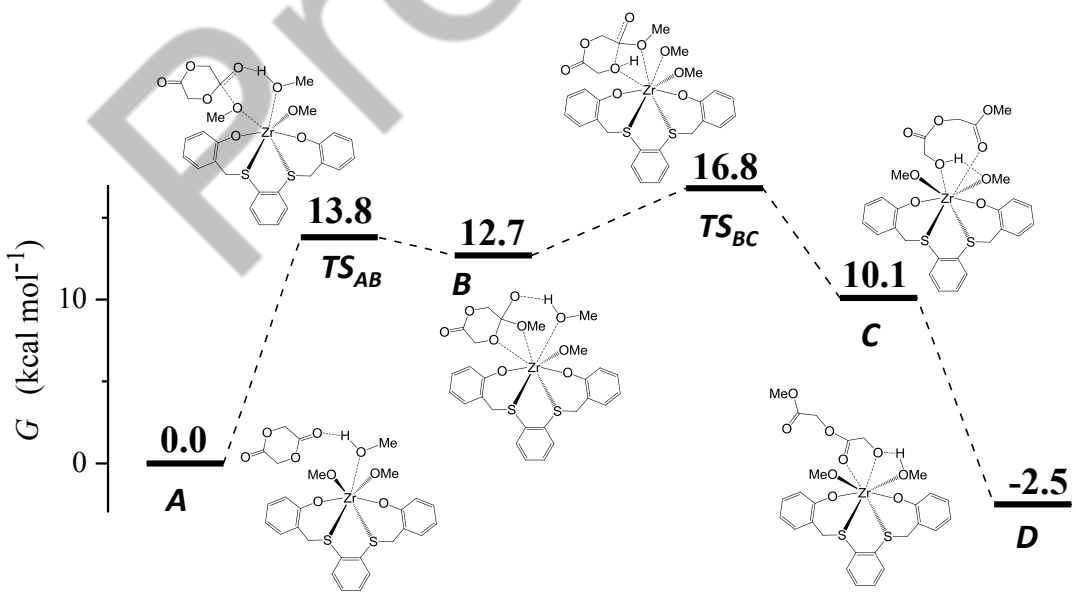

Figure 10. Computed free energy surface for the ring opening polymerization of glicolide promoted by zirconium model complex and methanol. The free energies are given in kcal/mol.

Pre-print

Inorg. Chem. 2017, 56, 3447−3458 DOI: 10.1021/acs.inorgchem.6b02987

It is worth noting that, in the mechanism we disclosed here, alcohol does not externally attack the metal bound monomer, as it generally assumed for the "activated monomer" mechanism.[19] In our case the nucleophilc attack at the carbon atom of the C=O is carried out by the alkoxyde ligand bounded to the metal centre, that is coherent with the higher nucleophilic character of the alkoxide anion compared to the neutral alcohol. Moreover alcohol behaves as a source of proton stabilizing the negatively charged intermediates that form after the nucleophilic attack to the ester group and facilitating the subsequent ring opening step.

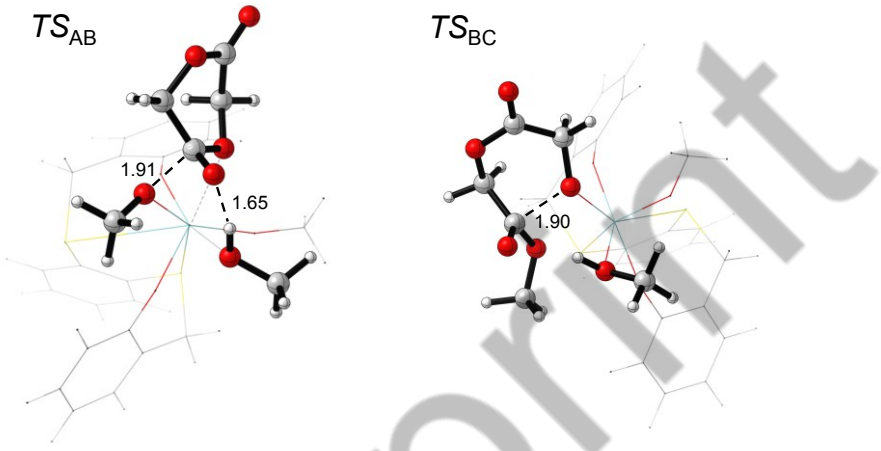

Figure 11. Transition states for the nucleophilic attack (TS_{AB}) and ring opening (TS_{BC}) for the zirconium model complex. Distances are given in Å.

Pre-print

Conclusions

A series of group 4 metal complexes supported by *orto*-phenylene-bridged bis(phenolato) ligands were successful synthesized and fully characterized by NMR spectroscopy. In one case X-ray crystallographic data were obtained and confirmed the *fac-fac* ligand wrapping around the metal center. The zirconium and hafnium complexes resulted configurationally stable, the barriers for the inversion of configuration at the metal center, obtained from EXSY experiments, were proportional to the bulk of the substituents on the phenolate rings. The titanium complex was substantially more flexible than the analogous complexes, probably cause of the weaker interaction between the soft sulfur atom and the hard titanium ion.

In the ring opening polymerization of rac-lactide, all complexes, except the homoleptic derivative **3**, displayed moderate rates and good polymerization control. As matter of fact linear dependences of M_n versus the percentage conversion and narrow molecular weight distributions were observed. Although the end group analysis indicated that the polymerization is started by the transfer of the metal-bound alkoxide group bound to the monomer, the presence of an induction

Inorg. Chem. 2017, 56, 3447−3458 DOI: 10.1021/acs.inorgchem.6b02987

period at the begin of the reaction suggests that the initiators undergo a drastic change before the polymerization can start.

In the presence of exogenous alcohol, all complexes displayed higher rates. Moreover the linear evolution of molecular weight as the polymerization progresses, the narrow polydispersity indices, and the molecular weights corresponding to those predicted on the basis of added alcohol equivalents demonstrate that adequate conditions for effective "immortal" polymerizations were achieved. The lack of reactivity of these complexes with exogenous alcohol has induced us to proposed that these compounds operate by an activated monomer mechanism. This conclusion was also support by DFT studies that failed to locate the coordination adduct between the monomer and the zirconium model complex. It is well know that in the coordination insertion mechanism the monomer coordination to the metal center is a prerequisite for the insertion of the monomer in the Metal-alkoxide bond. Moreover a plausible reaction path for the activated monomer mechanism was proposed.

Herein we demonstrated for the first time that the ROP reactions catalyzed by binary systems based on group IV complexes follow an activated monomer mechanism and not the classical coordination–insertion commonly asserted for related systems.

Pre-print

Experimental part

Materials and methods. All preparations and subsequent manipulations of air- and/or water-sensitive compounds were carried out under a dry nitrogen atmosphere using a Braun Labmaster drybox or standard Schlenk line techniques. Glassware and vials used in the polymerization were dried in an oven at 120 °C overnight and exposed three times to vacuum-nitrogen cycles. All solvents and reagents used were dried and purified before use. Toluene (Sigma-Aldrich, 99.5%), hexane (Sigma-Aldrich, 99%) were preliminarily dried over $CaCl_2$, while THF (Sigma-Aldrich, 99%) was preliminarily treated with potassium hydroxide. Then, all solvents were purified by distillation from sodium under a nitrogen atmosphere. Ligands used for the synthesis of complexes were anhydrificated in vacuum with P_2O_5. Lactide was purified by crystallization from dry toluene and then stored over P_2O_5. 2-Propanol and tert-butanol were dried and distilled over magnesium turnings and stored over 4Å molecular sieves. Deuterated solvents were dried using molecular sieves. All other chemicals were commercially available and used as received unless otherwise stated.

Inorg. Chem. 2017, 56, 3447−3458 DOI: 10.1021/acs.inorgchem.6b02987

Instruments and Measurements. The NMR spectra were recorded on Bruker Avance 400 spectrometer (^{1}H, 400.01 MHz; ^{13}C, 100.62 MHz) at 25 °C, unless otherwise stated. Deuterated solvents were purchased from Cambridge Isotope Laboratories, Inc., degassed and dried over activated 3Å molecular sieves prior to use. Chemical shifts (δ) are listed as parts per million and coupling constants (*J*) in hertz. ^{1}H NMR spectra are referenced using the residual solvent peak at δ 7.16 for C_6D_6, δ 7.27 for $CDCl_3$ and δ 5.32 for CD_2Cl_2. ^{13}C NMR spectra are referenced using the residual solvent peak at δ 128.39 for C_6D_6, δ 77.23 for $CDCl_3$ and δ 53.84 for CD_2Cl_2. Variable temperature ^{1}H NMR experiments were recorded with Bruker Avance 600 spectrometer in toluene-d_8 using J-Young NMR tube.

The 2D EXSY spectra were recorded at 333 K in C_6D_6 for **1**, **2** and **5** and in $CDCl_3$ for **3** at different mixing times (300-700 ms). The rate constants (*k*) were calculated employing the equations reported below,[20] in which *k*' is the sum of the forward and reverse reaction rates, τ_ω is the mixing time, I_{AB} and I_{BA} are the cross-peak intensities, I_{AA} and I_{BB} are the diagonal peak intensities:

$$k' = 1/\ \tau_\omega \ln[(r+1)/(r-1)]$$
$$r = 4\ (I_{AA} + I_{BB})/(I_{AB} + I_{BA})$$

Because the forward and reverse rate constants are equal in these cases, the rate for the Λ-Δ interconversion is given by $k = k'/2$. The free energy of activation ($\Delta G^{\#}$) was calculated using the equation $\Delta G^{\#} = -RT \ln kh/TK_B$.

Variable-temperature NMR study for **4** was performed with a Bruker ASCEND 600 in CD_2Cl_2 using 5mm NMR tubes equipped J Young valves. The chemical shifts are referred to tetramethylsilane as an external standard. The analysis was referred to the methylene protons of the $OSSO_{Cum}$ ligand that consist in a simple two spin (not coupled) system and produce two singlets in the slow exchange regime at -50 °C (Figure S13). NMR simulations were performed using DNMR module of Topspin 3.0 (BRUKER). Final simulated line shapes were obtained via an iterative parameter search upon the exchange constant *k*. The activation parameters $\Delta H^{\#}$ and $\Delta S^{\#}$ were determined from the inverse temperature plot of ln(*k*/T). Estimated standard deviations (σ) in the slope and y-intercept of the Eyring plot determined the error in $\Delta H^{\#}$ and $\Delta S^{\#}$, respectively. The standard deviation in $\Delta G^{\#}$ was determined from the formula: $\sigma(\Delta G^{\#})^2 = \sigma(\Delta H^{\#})^2 + [T\ \sigma(\Delta S^{\#})]^2 – 2T\ \sigma(\Delta H^{\#})\sigma(\Delta S^{\#})$.

In the case of polylactide samples obtained from the polymerization of *rac*-LA, the evaluation of the probability to obtain an *r* diad (P_r) was made by the analysis of the relative intensities of the

Pre-print

Inorg. Chem. 2017, 56, 3447−3458 DOI: 10.1021/acs.inorgchem.6b02987

tetrads signals of the ^{1}H NMR homonuclear decoupled spectrum ($CDCl_3$, 300 MHz, ppm): *mrm* (5.16), *mmm* (5.17), *mmr*/*rmm* (5.18 and 5.22), and *rmr* (5.23).[17] Electrospray ionization mass spectra were acquired using a Micromass Quattro micro API triple quadrupole mass spectrometer equipped with an electrospray ion source (Waters, Milford, MA). Acetonitrile was added to the samples, and the solutions were continuously infused into the electrospray ionization (ESI) ion source at a rate of 10 μL/min using the instrument syringe pump. The LCQ ion source was operating at 4 kV, and the capillary heater was set to 100 °C. Nitrogen was used as nebulizing gas, and nitrogen was used as damping gas and collision gas in the mass analyzer. Positive ion mode was used for all analyses. No cationizing agents were used for ESI measurements because K^+, Na^+, and H^+ adduct ions were detectable at high intensity. The origin of these alkali metals was apparently the ambient contaminants. The molecular weights (M_n and M_w) and the molecular mass distribution (M_n/M_w) of polymer samples were measured by gel permeation chromatography (GPC) at 30 °C, using THF as solvent, flow rate of eluent 1 mL/min, and narrow polystyrene standards as reference. The measurements were performed on a Waters 1525 binary system equipped with a Waters 2414 RI detector using four Styragel columns (range 1000–1000000 Å). Every value was the average of two independent measurements. It was corrected using the factor of 0.58 for polylactide according to the literature.[21]

Synthesis of the pro-ligands. The OSSO ligands used in this work were prepared by nucleophilic substitution of the suitable 2-(bromomethyl)-phenol with benzene-1,2-dithiol using a modified literature procedure.[12,22]

Synthesis of 2-(bromomethyl)-4,6-bis(2-phenylpropan-2-yl)phenol. In a round-bottomed flask, equipped with a magnetic stirrer, 2,4-bis(2-phenylpropan-2-yl)phenol (10.0 g, 30.3 mmol) was dissolved in acetic glacial acid (c.a. 100 mL) and paraformaldehyde (1.0 g, 33.3 mmol, 1.1 eq.) was added. The reaction mixture was stirred for 2 h at room temperature. Then, a solution of HBr 33% in acetic acid (34 mL, 194.3 mmol, 6.4 eq) was added dropwise and the resulting yellow solution was stirred for 90 minutes. After stirring, the reaction mixture was poured into a cold bath (T= 0°C) and extracted with CH_2Cl_2 (3x50 mL). The organic solvent was removed in vacuum and the orange viscous oil was obtained. Finally, the crude oil was dissolved in petroleum ether (10 mL) and stored at -20 °C overnight. The desired product was collected as a white solid (77% yield). Spectroscopic data: ^{1}H NMR (300 MHz, $CDCl_3$, 25°C) = δ 7.37-7.25 (m, 9H, CH_{Ph} + 1H CH_{Ar}), 7.22-7.18 (m, 1H, CH_{Ph}), 7.14 (d, J_{HH} = 2.2 Hz, 1 H, CH_{Ar}), 4.60 (br, 1H, OH), 4.45 (s, 2H, CH_2), 1.75 (s, 6H, $C(CH_3)_2Ph$), 1.63 (s, 6H, $C(CH_3)_2Ph$). ^{13}C NMR (75.4 MHz, $CDCl_3$, 25 °C) = δ 150.8, 150.3, 147.9, 142.7 and 135.4 (C_{ipso} Ar + Ph), 129.5 and 128.2 (CH_{Ph}), 127.8 and 127.5 (CH_{Ar}), 126.9, 126.2,

Pre-print

Inorg. Chem. 2017, 56, 3447−3458 DOI: 10.1021/acs.inorgchem.6b02987

126.1 and 125.9 (CH_{Ph}), 125.4 (C_{ipso} Ar or Ph), 42.8 and 42.1 ($C(CH_3)_2Ph$), 31.2 ($C(CH_3)_2Ph$), 30.5 (CH_2), 29.8 ($C(CH_3)_2Ph$).

Synthesis of 6,6'-((1,2-phenylenebis(sulfanediyl)bis(methylene))bis(2,4-di-phenylpropan-2-yl)phenol) ($OSSO_{Cum}$-H). In a round-bottomed flask, equipped with a magnetic stirrer, 1,2-benzenedithiol (0.50 g, 3.51 mmol) was dissolved in THF dry (10 mL). Then, a solution of sodium *tert*-butoxide (0.68 g, 7.08 mmol, 2 eq.) in 20 mL of THF dry was added dropwise to the dithiol solution. The subsequent formation of sodium salt was evident, when the reaction mixture appeared as a white suspension. Finally, a THF solution (20 mL) of 2-(bromomethyl)-4,6-bis(2-phenylpropan-2-yl)phenol was added to the mixture and the reaction was carried out overnight at room temperature. The solvent was distilled off, water was added until dissolution of NaBr by-product and the aqueous phase extracted twice with methylene chloride. The combined organic phases were dried with Na_2SO_4 and, after evaporation of the solvent, the resulting crude oil was purificated by crystallization in petroleum ether at room temperature. The ligand is an off-white solid. 78% yield. Single crystals were grown from toluene/THF (1:1 v/v). Spectroscopic data: ^{1}H NMR (300 MHz, $CDCl_3$, 25°C) = δ 7.32-7.25 (m, 10 H), 7.19 (m. 10 H), 7.01 (m, 4 H), 6.86 (m, 2H), 4.88 (s, br, 2H, OH), 3.96 (s, 4H, CH_2), 1.61 (s, 24 H, CH_3). ^{1}H NMR (250 MHz, C_6D_6, 25°C) = δ 7.51-7.39 (m, 14H), 7.34-7.31 (m, 8H), 7.01 (d, 2H), 5.03 (s,2H, OH), 4.11 (s, 4H, CH_2), 1.76 (s, 24 H, CH_3). ^{13}C NMR (62.9 MHz, C_6D_6, 25°C) = δ 202.40, 201.39, 200.27, 193.23, 188.32, 186.59, 182.38, 180.23, 179.25, 178.92, 178.05, 177.27, 176.81, 176.00, 174.85, 93.82 (CH), 93.29 (CH), 85.11 (CH_2), 82.30 (CH_3), 80.99 (CH_3). Elemental analysis calcd (%) for $C_{56}H_{58}O_2S_2$: C, 81.31; H, 7.07; S, 7.75. Found: C, 81.58; H, 7.29; S, 7.51. $[M + Na]^+$ = 848.9 m/z

Synthesis of 6,6'-((1,2-phenylenebis(sulfanediyl)bis(methylene))bis(2,4-di-tert-butyl-2-yl)phenol) ($OSSO_{tBu}$-H). The synthesis of $OSSO_{tBu}$-*H* was performed according to the same procedure as for $OSSO_{Cum}$-*H*. Yield: 75%. ^{1}H NMR (250 MHz, $CDCl_3$, 25 °C) = δ 7.37-7.33 (m, 2H), 7.22 (d, 2H), 7.16-7.10 (m, 2H), 6.87 (d, 2H), 6.10 (s, 2H, OH), 4.14 (s, 4H, CH_2), 1.42 (s, 18H, CH_3), 1.22 (s, 18H, CH_3). ^{1}H NMR (250 MHz, C_6D_6, 25°C) = δ 7.39 (m, 2H), 7.10-7.06 (t, 2H), 6.84 (s, 2H, OH), 6.71-6.59 (t, 2H), 6.27 (d, 2H), 3.82 (s, 4H, CH_2), 1.57 (s, 18H, CH_3), 1.23 (s, 18H, CH_3). ^{13}C NMR (75.4 MHz, $CDCl_3$, 25°C) = δ 152.48, 142.90, 137.75, 137.73, 133.51, 128.71, 126.17, 124.33, 122.56, 37.58 (CH), 35.65 (CH), 34.66 (CH_2), 32.06 (CH_3), 30.46 (CH_3). $[M + Na]^+$ = 601.7 m/z

Synthesis of 6,6'-((1,2-phenylenebis(sulfanediyl)bis(methylene))bis(2,4-di-chloro-2-yl)phenol) ($OSSO_{Cl}$-H). The synthesis of $OSSO_{Cl}$-*H* was performed according to the same procedure as for $OSSO_{Cum}$-*H*. Yield: 50%. Spectroscopic data: ^{1}H NMR (300 MHz, $CDCl_3$, 25 °C) = δ 7.27-7.24 (m, 4H), 7.19-715 (m, 2H), 7.02 (d, 2H), 5.87 (s, br, OH), 4.11 (s, 4H, CH_2). ^{1}H NMR (250 MHz, C_6D_6, 25°C) = δ 7.05-7.01 (m, 2H), 6.88-6.84 (dd, 4H), 6.77-6.73 (m, 2H), 5.50 (s, 2H, OH), 3.78 (s, 4H,

Pre-print

Inorg. Chem. 2017, 56, 3447−3458 DOI: 10.1021/acs.inorgchem.6b02987

CH2). ^{13}C NMR (62.9 MHz, C_6D_6, 25°C) = δ 149.19, 137.87, 131.69, 129.72, 128.18, 127.90, 126.96, 125.68, 121.34, 334.45. Elemental analysis calcd (%) for $C_{20}H_{14}Cl_4O_2S_2$: C, 48.80; H, 2.87; S, 13.03. Found: C, 48.94; H, 2.96; S, 12.94. $[M + Na]^+$ = 515.2 m/z

Synthesis of ($OSSO_{tBu}$)Zr(O^tBu)$_2$ (1). A solution of Zr(O^tBu)$_4$ (0.86 mmol, 0.33 g) in toluene (5 mL) was added to a stirred solution of $OSSO_{tBu}$-*H* (0.86 mmol, 0.50 g) in toluene (5 mL) at room temperature. The resulting pale yellow solution was stirred for 2 h after which the volatiles were removed in vacuum. The crude product was washed with hexane to give **1** as a yellow solid (0.46 g, 66 %) that was pure according to ^{1}H NMR and elemental analysis. Spectroscopic data: ^{1}H NMR (600 MHz, Tol-d_8, 25°C) = δ 7.29 (d, 2H), 6.90-6.88 (m, 2H), 6.66-6.63 (m, 2H), 6.06 (d, 2H), 4.19 (d, 2H, CH_2), 3.30 (d, 2H, CH_2), 1.77 (s, 18H, CH_3), 1.57 (s, 18H, CH_3), 1.08 (s, 18H, CH_3). ^{13}C NMR (75.4 MHz, CD_2Cl_2, 25°C) = δ 159.81, 139.05, 137.57, 136.71, 136.39, 130.55, 126.04, 123.95, 121.17, 77.47, 53.98, 41.96, 35.71, 33.17, 33.00, 31.83, 30.86. Elemental analysis calcd (%) for $C_{44}H_{66}O_4S_2Zr$: C, 64.90; H, 8.17; S, 7.88. Found: C, 65.05; H, 8.19; S, 7.84.

Synthesis of ($OSSO_{Cum}$)Zr(O^tBu)$_2$ (2). ($OSSO_{Cum}$)Zr(O^tBu)$_2$ was prepared in high yield (70%) from $OSSO_{Cum}$-*H* (0.500 g, 0.604 mmol) and Zr(O^tBu)$_4$ (0.232 g, 0.604 mmol) as described above for ($OSSo_{tBu}$)Zr(O^tBu)$_2$ (**1**). ^{1}H NMR (600 MHz, Tol-d_8, 25°C) = δ 7.38-7.36 (m, 4H), 7.19-7.04 (m, 18H), 6.94-6.88 (m, 2H), 6.72-6.70 (m, 2H), 5.95 (d, 2H), 4.00 (d, 2H, CH_2), 3.13 (d, 2H, CH_2), 2.19 (s, 6H, CH_3), 1.71 (s, 6H, CH_3), 1.39 (s, 12H, CH_3), 1.33 (s, 18H,CH_3). ^{13}C NMR (75.4 MHz, CD_2Cl_2, 25°C) = δ 151.60, 150.59, 149.57, 142.46, 137.43, 135.74, 131.53, 129.33, 128.40, 128.17, 127.31, 127.22, 127.02, 126.47, 125.94, 125.13, 124.13, 69.34, 42.97, 42.46, 34.22, 31.55, 31.24, 29.95. Elemental analysis calcd (%) for $C_{64}H_{74}O_4S_2Zr{\cdot}C_7H_8$: C, 73.85; H, 7.16; S, 5.55. Found: C, 73.70; H, 7.14; S, 5.56.

Synthesis of ($OSSO_{Cl}$)$_2$Zr (3). A solution of Zr(O^tBu)$_4$ (0.50 mmol, 0.19 g) in toluene (5 mL) was added to a stirred solution of $OSSO_{Cl}$-*H* (1.01 mmol, 0.50 g) in toluene (5 mL) at room temperature. The resulting pale yellow solution was stirred for 2 h after which the volatiles were removed in vacuum. The crude product was washed with hexane to give **1** as a yellow solid (0.62 g, 57%) that was pure according to ^{1}H NMR and elemental analysis. Spectroscopic data: ^{1}H NMR (600 MHz, Tol-d_8, 25°C) = δ 7.04 (d, 4H), 6.75-6.73 (m, 4H), 6.60-6.58 (m, 4H), 5.88 (d, 4H), 5.59 (d, 4H, 2CH_2), 3.19 (d, 4H, 2CH_2). ^{13}C NMR (74.5 MHz, CD_2Cl_2, 25°C) = δ 157.40, 136.66, 135.52, 131.08, 129.10, 127.83, 126.95, 124.61, 122.70, 41.40.

Elemental analysis calcd (%) for $C_{40}H_{24}Cl_8O_4S_4Zr$: C, 44.83; H, 2.26; S, 11.97. Found: C, 44.92; H, 2.28; S, 11.93.

Synthesis of ($OSSO_{Cum}$)Ti(O^iPr)$_2$ (4). A solution of Ti(O^iPr)$_4$ (0.47 mmol, 0.17 g) in toluene (5 mL) was added to a stirred solution of $OSSO_{Cum}$-*H* (0.47 mmol, 0.50 g) in toluene (5 mL) at room

Pre-Print

Inorg. Chem. 2017, 56, 3447−3458 DOI: 10.1021/acs.inorgchem.6b02987

temperature. The resulting pale yellow solution was stirred for 2 h after which the volatiles were removed in vacuum. The crude product was washed with hexane to give **1** as a yellow solid (0.30 g, 64%) that was pure according to ^{1}H NMR and elemental analysis. Spectroscopic data: ^{1}H NMR (600 MHz, CD_2Cl_2, 25°C) = δ 7.34-7.33 (m, 2H), 7.24-7.04 (m, 20H), 6.89-6.87 (m, 4H), 6.03 (d, 2H), 4.38 (m, 2CH), 3.61 (s, broad, 4H, $2CH_2$), 1.78 (s, broad, 12H, $4CH_3$), 1.38 (s, 12H, $4CH_3$), 1.05 (d, 12H, $4CH_3$).^{13}C NMR (62.9 MHz, CD_2Cl_2, 25°C) = δ 161.42, 152.44, 151.98, 138.91, 137.65, 137.58, 135.46, 130.52, 128.18, 127.69, 127.64, 127.02, 126.80, 125.88, 125.56, 125.03, 122.00, 79.40, 42.60, 41.18, 31.13, 25.99. Elemental analysis calcd (%) for $C_{62}H_{70}O_4S_2Ti$: C, 75.13; H, 7.12; S, 6.47. Found: C, 75.29; H, 7.14; S, 6.44.

Synthesis of ($OSSO_{Cum}$)Hf(O^tBu)$_2$ (5). A solution of Hf(O^tBu)$_4$ (0.47 mmol, 0.22 g) in toluene (5 mL) was added to a stirred solution of $OSSO_{Cum}$-*H* (0.47 mmol, 0.50 g) in toluene (5 mL) at room temperature. The resulting pale yellow solution was stirred for 2 h after which the volatiles were removed in vacuum. The crude product was washed with hexane to give **1** as a yellow solid (0.37 g, 68%) that was pure according to ^{1}H NMR and elemental analysis. Single crystals of the complex were grown from toluene at -20 °C. Spectroscopic data: ^{1}H NMR (600 MHz, Tol-d_8, 25°C) = δ 7.38-7.36 (d, 2H), 7.15-7.13 (q, 2H), 7.07-6.92 (m, 20H), 6.75-6.73 (m, 2H), 5.95 (d, 2H), 4.05 (d, 2H, CH_2), 3.20 (d, 2H, CH_2), 2.14 (s, 6H, CH_3), 1.74 (s, 6H, CH_3), 1.36 (s, 12H, CH_3), 1.33 (s, 18H,CH_3). ^{13}C NMR (75.4 MHz, CD_2Cl_2, 25°C) = δ 159.47, 152.37, 152.04, 138.22, 138.02, 136.78, 136.46, 130.76, 128.17, 127.83, 127.03, 126.84, 125.54, 125.18, 121.30, 76.85, 42.91, 42.41, 41.66, 33.10, 32.79, 31.42, 30.85, 28.29. Elemental analysis calcd (%) for $C_{64}H_{74}HfO_4S_2$: C, 66.85; H, 6.49; S, 5.58. Found C, 66.97; H, 6.51; S, 5.54.

Lactide polymerizations. In a typical polymerization, in a glovebox, a Schlenk flask (10 cm^3) was charged sequentially with *rac*-lactide, (0.180 g, 1.25 mmol), and the precatalyst (12.5 μmol) dissolved in 2,4 mL of dry toluene. The mixture was thermostated at the required temperature. At specified time intervals, a small amount of the polymerization mixture was sampled by a pipette and quenched in wet $CDCl_3$ to evaluate the yields. This fraction was subjected to monomer conversion determination, which was monitored by integration of monomer versus polymer methine resonances in ^{1}H NMR spectrum ($CDCl_3$). After the required polymerization time, the reaction mixture was quenched with wet *n*-hexane. The precipitates collected from the bulk mixture were dried in air, dissolved with dichloromethane, and sequentially precipitated into methanol. The obtained polymer was collected by filtration and further dried in a vacuum oven at 40 °C for 16 h. The polymer was characterized by NMR spectroscopy and GPC analysis. The chemical shifts of polylactide are 1.64 (d, 6H, –CHC*H*$_3$–), 5.18 (q, 2H, –C*H*CH$_3$–). The chemical shifts of lactide are 1,59 (d, 6H, –CHC*H*$_3$–), 4.85 (t, 2H, –C*H*CH$_3$–).

Pre-print

Inorg. Chem. 2017, 56, 3447−3458 DOI: 10.1021/acs.inorgchem.6b02987

Lactide polymerizations in presence of alcohol. In a typical polymerization, in a glovebox, a Schlenk flask (10 cm^3) was charged sequentially with rac-lactide (0.180 g, 1.25 mmol), and the precatalyst (12.5 μmol) dissolved in proper amount of dry toluene to reach a total volume of 2.4 mL. Subsequently, 0.30, 0.75 or 1.5 mL of a 0.083 M solution of alcohol (isopropanol or tertbutanol) in toluene (25, 62.5 or 125 μmol) was added. The volume was kept constant to 2.4 mL. The mixture was thermostated at the required temperature. At specified time intervals, a small amount of the polymerization mixture was sampled by a pipette and quenched in wet $CDCl_3$ to evaluate the yields. This fraction was subjected to monomer conversion determination, which was monitored by integration of monomer versus polymer methine resonances in ^1H NMR spectrum ($CDCl_3$). After the required polymerization time, the reaction mixture was quenched with wet *n*-hexane. The precipitates collected from the bulk mixture were dried in air, dissolved with dichloromethane, and sequentially precipitated into methanol. The obtained polymer was collected by filtration and further dried in a vacuum oven at 40 °C for 16 h. The polymer was characterized by NMR spectroscopy and GPC analysis.

Computational details. Density functional theory (DFT) calculations were performed with the program suite Gaussian 09.[23] All geometries were optimization without constraints at the BP86 level, i.e., employing the exchange and correlation functionals of Becke and Perdew,[24] respectively. The basis set employed was the LANL2DZ[25] with associate effective core potentials for Zr and S and 6-31G(d) for O, C, and H. Geometry optimizations were performed without symmetry constraints. Stationary point geometries were characterized as local minimum on the potential energy surfaces. The absence of imaginary frequency verified that structures were true minima at their respective levels of theory. The structure of transition state were located by applying Schlegel's synchronous-transit-guided quasi-Newton (QST2) method as implemented in GAUSSIAN 09. The transition states were verified with frequency calculations to ensure they were first order saddle points with only one negative eigenvalue. Cartesian coordinates of all DFT optimized structures are available on request. Structures were visualized by the CYLview program.[26]

Single Crystal X-ray crystallography

A suitable crystal of **$(OSSO_{Cum})Zr(O^tBu)_2 \bullet C_7H_8$** was mounted on a goniometer head and cooled to 100 K in a stream of cold N_2 using Bruker Kryoflex low temperature device whereas the **$OSSO_{Cum}$-H** ligand was mounted on a goniometer head and kept at room temperature.The X-ray intensity data for both structures were measured on a Bruker SMART Apex II CCD area detector diffractometer. Cell dimensions and the orientation matrix were initially determined from a least-squares refinement on reflections measured in three sets of 20 exposures, collected in three different ω

Pre-print

Inorg. Chem. 2017, 56, 3447−3458 DOI: 10.1021/acs.inorgchem.6b02987

regions, and eventually refined against all data. A full sphere of reciprocal space was scanned by 0.3° ω steps. The software SMART[27] was used for collecting frames of data, indexing reflections, and determination of lattice parameters. The collected frames were then processed for integration by the SAINT program and an empirical absorption correction was applied using SADABS.[28] The structures were solved by direct methods (SIR 2004)[29] and subsequent Fourier syntheses and refined by full-matrix least-squares on F^2 (SHELXTL)[30], using anisotropic thermal parameters for all non-hydrogen atoms. All hydrogen atoms were added in calculated positions, included in the final stage of refinement with isotropic thermal parameters, U(H) = 1.2 U_{eq}(C) [U(H) = 1.5 U_{eq}(C-Me)], and allowed to ride on their carrier carbons. In the asymmetric unit of **$(OSSO_{Cum})Zr(O^tBu)_2$• C_7H_8** a toluene solvent molecule is present. Three methyl groups of one tert-butyloxy moiety are disordered over two positions with occupation factors of 78 and 22%, respectively.

Crystal data and details of the data collection for **$(OSSO_{Cum})Zr(O^tBu)_2$• C_7H_8** and **$OSSO_{Cum}$-H** are reported in Table **3**. CCDC 1517665 and CCDC 1517664 contains the supplementary crystallographic data for this paper. These data can be obtained free of charge from the Cambridge Crystallographic Data Centre via www.ccdc.cam.ac.uk/data_request/cif.

Pre-print

Table 3. Crystal data and structure refinement for **$OSSO_{Cum}$-H** and **$(OSSO_{Cum})Zr(O^tBu)_2$ • C_7H_8** .

	$OSSO_{Cum}$-H	**$(OSSO_{Cum})Zr(O^tBu)_2$**
Empirical formula	$C_{56}H_{58}O_2S_2$	$C_{64}H_{74}O_4S_2Zr•C_7H_8$
Formula weight	827.14	1154.70
Temperature/K	296(2)	100(2)
Crystal system	Triclinic	Triclinic
Space group	P -1	P -1
a, Å	12.7680(7)	12.2584(8)
b, Å	13.8560(8)	13.0961(8)
c, Å	14.8684(8)	20.3390(13)
α, °	68.673(3)	97.925(3)
β, °	76.025(3)	101.671(3)
γ, °	75.630(3)	98.390(3)
Cell volume, $Å^3$	2340.1(2)	3115.9(3)
Z	2	2
ρ_c, mg m^{-3}	1.174	1.231

Inorg. Chem. 2017, 56, 3447−3458 DOI: 10.1021/acs.inorgchem.6b02987

μ(Mo-K_α), mm^{-1}	0.155	0.291
F(000)	884	1228
Crystal size mm	0.30 x 0.25 x 0.15	0.20 x 0.20 x 0.15
θ limits, °	1.491 to 25.126	1.038 to 24.927
Refl. collected, unique (R_{int})	34094 / 8256 (0.0286)	43666 / 10765 (0.0318)
Goodness-of-fit-on F^2	0.995	1.046
$R_1(F)^a$, $wR_2(F^2)$ $[I > 2\sigma(I)]^b$	0.0407, 0.100	0.0265, 0.0659
Largest diff. peak and hole, e. $Å^{-3}$	0.230 and -0.210	0.345, -0.361

[a] $R_1 = \Sigma||F_o|-|F_c||/\Sigma|F_o|$. [b] $wR_2 = [\Sigma w(F_o^2-F_c^2)^2/\Sigma w(F_o^2)^2]^{1/2}$ where $w = 1/[\sigma^2(F_o^2) + (aP)^2 + bP]$ where $P = (F_o^2+F_c^2)/3$.

Acknowledgements

The authors thank Dr. Patrizia Oliva and Dr. Patrizia Iannece for technical assistance. Financial support is acknowledged from the Ministero dell'Istruzione dell'Università e della Ricerca (MIUR, Roma, Italy for FARB 2015) and the SPRING cluster (REBIOCHEM research project CTN01_00063_49393). The Centro di Tecnologie Integrate per la Salute (Project PONa3_00138) for the 600 MHz NMR instrumental time is acknowledged.

Supporting Information Available: Figures giving ^{1}H NMR spectra of proligands and complexes, plots of number-averaged molecular *vs* monomer conversion, pseudo-first-order kinetic plots, and crystallographic data for complex **2**. This material is available free of charge via the Internet at http://pubs.acs.org.

Pre-print

Inorg. Chem. 2017, 56, 3447−3458 DOI: 10.1021/acs.inorgchem.6b02987

References

1) (a) Ragauskas, A. J.; Williams, C. K.; Davison, B. H.; Britovsek,G.; Cairney, J.; Eckert, C. A.; Frederick, W. J.; Hallett, J. P.; Leak, D. J.;Liotta, C. L.; Mielenz, J. R.; Murphy, R.; Templer, R.; Tschaplinski, T. The Path Forward for Biofuels and Biomaterials. *Science* **2006**, *311*, 484−489. (b) Mecking, S. Nature or Petrochemistry?—Biologically Degradable Materials. *Angew. Chem., Int. Ed.* **2004**, *43*, 1078–1085 (c) Mülhaupt R. Green Polymer Chemistry and Bio-based Plastics: Dreams and Reality. *Macromol. Chem. Phys.* **2013**, *214*, 159-174. (d) Miller, S. A. Sustainable Polymers: Opportunities for the Next Decade. *ACS Macro Lett.*, **2013**, *2*, 550-554. (e) Tschan, M. J.-L.; Brulé, E.; Haquette, P.; Thomas, C. M. Synthesis of biodegradable polymers from renewable resources *Polym. Chem.*, **2012**, *3*, 836-851.

2) (a) Albertsson, A.-C.; Varma, I. K. Recent developments in ring opening polymerization of lactones for biomedical applications. *Biomacromolecules* **2003**, *4*,1466−1486 (b) Chiellini, E.; Solaro, R. Biodegradable Polymeric Materials. *Adv. Mater.* 1996, 8, 305−313. (c) Ikada, Y.; Tsuji, H. Biodegradable polyesters for medical and ecological applications. *Macromol. Rapid Commun.* **2000**, *21*, 117–132. (d) Auras, R.; Harte, B.; Selke, S. An overview of polylactides as packaging materials. *Macromol. Biosci.* **2004**, *4*, 835−864.

3) Dubois, P.; Coulembier, O.; Raquez, J.-M. *Handbook of Ring-Opening Polymerization*; Wiley-VCH: Weinheim, **2009**.

4) (a) Dijkstra, P. J.; Du, H.; Feijen, J. Single site catalysts for stereoselective ring-opening polymerization of lactides. *Polym. Chem.* **2011**, *2*, 520−527. (b) O'Keefe, B. J.; Hillmyer, M. A.; Tolman, W. B. Polymerization of lactide and related cyclic esters by discrete metal complexes. *J. Chem. Soc., Dalton Trans.* **2001**, 2215−2224. (c) Stanford, M. J.; Dove, A. P. Stereocontrolled ring-opening polymerisation of lactide. *Chem. Soc. Rev.* **2010**, *39*, 486−494. (d) Dechy-Cabaret, O.; Martin-Vaca, B.; Bourissou, D. Controlled Ring-Opening Polymerization of Lactide and Glycolide. *Chem. Rev.* **2004**, *104*, 6147−6176. (e) Thomas, C. M. Stereocontrolled ring-opening polymerization of cyclic esters: synthesis of new polyester microstructures. *Chem. Soc. Rev.* **2010**, *39*, 165−173. (f) Buffet, J. C.; Okuda, Initiators for the stereoselective ring-opening polymerization of meso-lactide. *J. Polym. Chem.* **2011**, *2*, 2758−2763.

5) Sauer, A.; Kapelski, A.; Fliedel, C.; Dagorne, S.; Kol, M.; Okuda, J. Structurally well-defined group 4 metal complexes as initiators for the ring-opening polymerization of lactide monomers. *Dalton Trans.* **2013**, *42*, 9007−9023.

6) (a) Jones, M. D. ; Hancock, S. L.; McKeown, P.; Schäfer, P. M.; Buchard, A.; Thomas, L. H.; Mahon, M. F; Lowe, J. P. Zirconium complexes of bipyrrolidine derived salan ligands for the isoselective polymerisation of rac-lactide. *Chem. Commun.* **2014**, *50*, 15967-15970. (b) Jones, M. D.; Brady, L.; McKeown, P.; Buchard, A.; Schäfer, P. M.; Thomas, L. H.; Mahon, M. F.; Woodman, T. J.; Lowe, J. Metal influence on the iso- and hetero-selectivity of complexes of bipyrrolidine derived salan ligands for the polymerisation of rac-lactide. *Chem. Sci.*, **2015**, *6*, 5034-5039.

7) Sergeeva, E.; Kopilov, J.; Goldberg, I.; Kol, M. Dithiodiolate Ligands: Group 4 Complexes and Application in Lactide Polymerization. *Inorg. Chem.* **2010**, *49*, 3977−3979.

8) (a) Buffet, J.-C.; Okuda, J. Group 4 metal initiators for the controlled stereoselective polymerization of lactide monomers. *Chem. Commun.* **2011**, *47*, 4796−4798. (b) Buffet, J.-C.; Martin, A. N.; Kol, M.; Okuda, J. Controlled stereoselective polymerization of lactide monomers by

Preprint

group 4 metal initiators that contain an (OSSO)-type tetradentate bis(phenolate) ligand. *Polym. Chem.* **2011**, *2*, 2378−2384.

9) Stopper, A.; Okuda, J.; Kol, M. Ring-Opening Polymerization of Lactide with Zr Complexes of {ONSO} Ligands: From Heterotactically Inclined to Isotactically Inclined Poly(lactic acid. *Macromolecules*, **2012**, *45*, 698–704.

10) A. Stopper, K. Press, J. Okuda, I. Goldberg and M. Kol, Zirconium Complexes of Phenylene-Bridged {ONSO} Ligands: Coordination Chemistry and Stereoselective Polymerization of rac-Lactide. *Inorg. Chem*., **2014**, *53*, 9140–9150.

11) (a) Della Monica, F.; Luciano, E.; Roviello, G.; Grassi, A.; Milione, S.; Capacchione, C. Group 4 Metal Complexes Bearing Thioetherphenolate Ligands. Coordination Chemistry and Ring-Opening Polymerization Catalysis. *Macromolecules* **2014**, *47*, 2830-2841. (b) Della Monica, F.; Luciano, E.; Buonerba, A.; Grassi, A.; Milione, S.; Capacchione, C. Poly(lactide-co-ε-caprolactone) copolymers prepared using bis-thioetherphenolate group 4 metal complexes: synthesis, characterization and morphology. *RSC Adv.* **2014**, *4*, 51262-51267. (c) Luciano, E.; Della Monica, F.; Buonerba, A.; Grassi, A.; Capacchione, C.; Milione, S. Polymerization of ethylene and propylene promoted by group 4 metal complexes bearing thioetherphenolate ligands. *Polym. Chem.* **2015**, *6*, 4657–4668. (d) Luciano, E.; Buonerba, A.; Grassi, A.; Milione, S.; Capacchione, C. Thioetherphenolate group 4 metal complexes in the ring opening polymerization of rac-β-Butyrolactone. *J. Polym. Sci. Part A* **2016**, *54*, 3132–3139. (e) Lapenta, R.; Mazzeo, M.; Grisi, F. Monoamidinate titanium complexes: highly active catalysts for the polymerization and copolymerization of L-lactide and ε-caprolactone. *RSC Adv.* **2015**, *5*, 87635-87644.

12) Si, G.; Zhang, L.; Han, B.; Duan, Z.; Li, B.; Dong, J.; Li, X.; Liu, B. Novel chromium complexes with a [OSSO]-type bis(phenolato) dianionic ligand mediate the alternating ring-opening copolymerization of epoxides and phthalic anhydride. *Polym. Chem.* **2015**, *6*, 6372-6377.

13) Cohen, A.; Yeori, A.; Goldberg, I.; Kol, M. Group 4 Complexes of a New [OSSO]-Type Dianionic Ligand. Coordination Chemistry and Preliminary Polymerization Catalysis Studies. *Inorg. Chem.* **2007**, *46*, 8114-8116.

14) (a) Cohen, A., Goldberg, I.; Venditto, V., Kol, M. Oscillating Non-Metallocenes – from Stereoblock-Isotactic Polypropylene to Isotactic Polypropylene via Zirconium and Hafnium Dithiodiphenolate Catalysts. *Eur. J. Inorg. Chem.* **2011**, 5219-5223; (b) Groysman, S., Sergeeva, E., Goldberg, I., Kol, M., Salophan Complexes of Group IV Metals. *Eur. J. Inorg. Chem.* **2005**, 2480-2485.

15) Sauer, A.; Buffet, J.-C.; Spaniol, T. P.; Nagae, H.; Mashima, K.; Okuda, J. Synthesis, Characterization, and Lactide Polymerization Activity of Group 4 Metal Complexes Containing Two Bis(phenolate) Ligands. *Inorg. Chem.* **2012**, *51*, 5764−5770.

16) Zelikoff, A. L.; Kopilov, J.; Goldberg, I.; Coates, G. W.; Kol, M. New facets of an old ligand: titanium and zirconium complexes of phenylenediamine bis(phenolate) in lactide polymerisation catalysis. *Chem. Commun.* **2009**, 6804–6806.

17) (a) Thakur, K. A. M.; Kean, R. T.; Zell, M. T.; Padden, B. E.; Munson, E. J. An alternative interpretation of the HETCOR NMR spectra of poly(lactide). *Chem. Commun*. **1998**, 1913−1914. (b) Thakur, K. A. M.; Kean, R. T.; Hall, E. S.; Kolstad, J. J.; Lindgren, T. A.; Doscotch, M. A.; Siepmann, J. I.; Munson, E. J. High-Resolution ^{13}C and ^{1}H Solution NMR Study of Poly(lactide).

Pre-print

Inorg. Chem. 2017, 56, 3447−3458 DOI: 10.1021/acs.inorgchem.6b02987

Macromolecules **1997**, *30*, 2422−2428. (c) Zell, M. T.; Padden, B. E.; Paterick, A. J.; Thakur, K. A. M.; Kean, R. T.; Hillmyer, M. A.; Munson, E. J. Unambiguous Determination of the ^{13}C and ^{1}H NMR Stereosequence Assignments of Polylactide Using High-Resolution Solution NMR Spectroscopy. *Macromolecules*, **2002**, *35*, 7700-7707.

18) Ajellal, N.; Carpentier, J.-F.; Guillaume, C.; Guillaume, S. M.; Helou, M.; Poirier, V.; Sarazina, Y.; Trifonov, A. Metal-catalyzed immortal ring-opening polymerization of lactones, lactides and cyclic carbonates. *Dalton Trans.*, **2010**, *39*, 8363–8376.

19) (a) Sarazin, Y.; Poirier, V; Roisnel, T; Carpentier, J.-F. Discrete, Base-Free, Cationic Alkaline-Earth Complexes – Access and Catalytic Activity in the Polymerization of Lactide. *Eur. J. Inorg. Chem.* **2010**, 22, 3423-3428. (b) Sarazin, Y.; Liu, B; Roisnel, T; Maron, L.; Carpentier, J.-F. Discrete, Solvent-Free Alkaline-Earth Metal Cations: Metal·Fluorine Interactions and ROP Catalytic Activity. *J. Am. Chem. Soc.* **2011**, *133*, 9069-9087.

20) Pons, M.; Millet, O. Dynamic NMR studies of supramolecular complexes. *Prog. Nucl. Magn. Reson. Spectrosc*. **2001**, 38, 267-281.

21) Biela, T.; Duda, A.; Penczek, S. Control of Mn, Mw/Mn, end-groups, and kinetics in living polymerization of cyclic esters. *Macromol. Symp*. **2002**, *183*, 1-10.

22) (a) Konkol, M.; Nabika, M.; Kohno, T.; Hino, T.; Miyatake, T. Synthesis, structure and α-olefin polymerization activity of group 4 metal complexes with [OSSO]-type bis(phenolate) ligands. *J. Organomet. Chem.* **2011**, *696*, 1792-1802. (b) Gendler, S.; Zelikoff, A. L.; Kopilov, J.; Goldberg, I.; Kol, M. Titanium and Zirconium Complexes of Robust Salophan Ligands. Coordination Chemistry and Olefin Polymerization Catalysis. *J. Am. Chem. Soc*., **2008**, *130*, 2144–2145

23) Frisch, M. J.; Trucks, G. W.; Schlegel, H. B.; Scuseria, G. E.; Robb, M. A.; Cheeseman, J. R.; Scalmani, G.; Barone, V.; Mennucci, B.; Petersson, G. A.; Nakatsuji, H.; Caricato, M.; Li, X.; Hratchian, H. P.; Izmaylov, A. F.; Bloino, J.; Zheng, G.; Sonnenberg, J. L.; Hada, M.; Ehara, M.; Toyota, K.; Fukuda, R.; Hasegawa, J.; Ishida, M.; Nakajima, T.; Honda, Y.; Kitao, O.; Nakai, H.; Vreven, T.; Montgomery, J. A., Jr.; Peralta, J. E.; Ogliaro, F.; Bearpark, M.; Heyd, J. J.; Brothers, E.; Kudin, K. N.; Staroverov, V. N.; Kobayashi, R.; Normand, J.; Raghavachari, K.; Rendell, A.; Burant, J. C.; Iyengar, S. S.; Tomasi, J.; Cossi, M.; Rega, N.; Millam, J. M.; Klene, M.; Knox, J. E.; Cross, J. B.; Bakken, V.; Adamo, C.; Jaramillo, J.; Gomperts, R.; Stratmann, R. E.; Yazyev, O.; Austin, A. J.; Cammi, R.; Pomelli, C.; Ochterski, J. W.; Martin, R. L.; Morokuma, K.; Zakrzewski, V. G.; Voth, G. A.; Salvador, P.; Dannenberg, J. J.; Dapprich, S.; Daniels, A. D.; Farkas, O.; Foresman, J. B.; Ortiz, J. V.; Cioslowski, J.; Fox, D. J. Gaussian 09, revision A.02; Gaussian, Inc.: Wallingford, CT, 2009.

24) a) Becke, A. D.; Density-functional exchange-energy approximation with correct asymptotic behavior. *Phys. Rev. A* **1988**, *38*, 3098–3100; b) Perdew, J. P.; Density-functional approximation for the correlation energy of the inhomogeneous electron gas. *Phys. Rev. B* **1986**, *33*, 8822–8824; c) Perdew, J. P.; Erratum: Density-functional approximation for the correlation energy of the inhomogeneous electron gas. *Phys. Rev. B* **1986**, *34*, 7406–7406.

25) Hay, P. J.; Wadt, W. R. Ab initio effective core potentials for molecular calculations. Potentials for the transition metal atoms Sc to Hg. *J. Chem. Phys.* **1985**, *82*, 270–283.

26) Legault, C. Y.; CYLview, v1.0b; Université de Sherbrooke, 2009; http://www.cylview.org

Pre-print

Inorg. Chem. 2017, 56, 3447−3458 DOI: 10.1021/acs.inorgchem.6b02987

27) SMART & SAINT Software Reference Manuals, version 5.051 (Windows NT Version), Bruker Analytical X-ray Instruments Inc.: Madison, WI, 1998.

28) Sheldrick, G. M. SADABS, Program for empirical absorption correction, University of Göttingen, Germany, **1996**.

29) Burla, M. C.; Caliandro, R.; Camalli, M.; Carrozzini, B.; Cascarano, G. L.; De Caro, L.; Giacovazzo, C.; Polidori, G.; Spagna, R. SIR2004: an improved tool for crystal structure determination and refinement. *J. Appl. Crystallogr.* **2005**, *38*, 381-388.

30) Sheldrick, G. M. SHELXTLplus (Windows NT Version) Structure Determination Package, Version 5.1. Bruker Analytical X-ray Instruments Inc.: Madison, WI, USA, **1998**

Pre-print

Inorg. Chem. 2017, 56, 3447−3458 DOI: 10.1021/acs.inorgchem.6b02987

For Table of Contents use only

Stereorigid OSSO-type Group 4 Metal Complexes in the Ring Opening Polymerization of *rac*-Lactide

Rosita Lapenta, Antonio Buonerba, Assunta De Nisi,[#] Magda Monari,[#] Alfonso Grassi, Stefano Milione,* Carmine Capacchione.

Department of Chemistry and Biology, University of Salerno, via Giovanni Paolo II, 132 Fisciano I-84084, Salerno, Italy.

Interuniversity Consortium Chemical Reactivity and Catalysis, CIRCC, via Celso Ulpiani 27, 70126 (BA), Italy

[#] *Dipartimento di Chimica G. Ciamician, Alma Mater Studiorum, Università di Bologna, via Selmi 2, Bologna, Italy*

Preprint

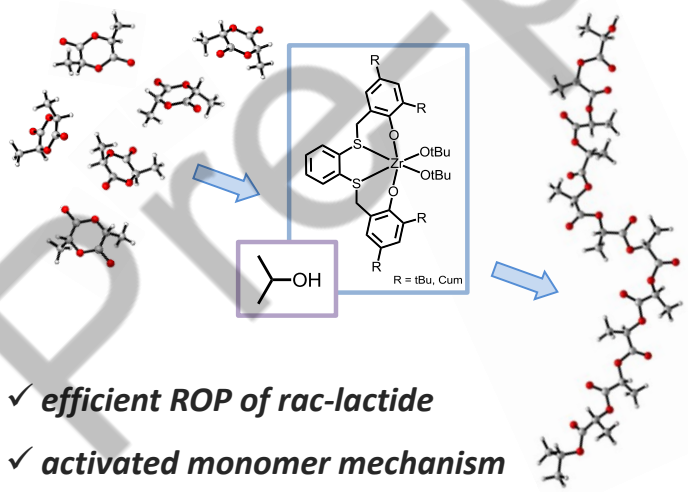

Group 4 metal complexes supported by stereorigid *ortho*-phenylene-bridged bis(phenolato) ligands mediate the immortal ROP of L-lactide yielding polymers with controlled molecular weight and narrow PDIs. It was shown for the first time that the ROP reactions catalyzed by group IV complexes in combination with exogenous alcohol may follow an activated monomer mechanism and not the classical coordination–insertion commonly asserted for related systems.